Hydrol. Earth Syst. Sci. Discuss., 9, 4305–4332, 2012
www.hydrol-earth-syst-sci-discuss.net/9/4305/2012/
doi:10.5194/hessd-9-4305-2012

Hydrology and Earth System Sciences Discussions

Comparison of heat tracer models in the estimation of upward flux through streambed sediments

M. Shanafield[1], **C. L. Shope**[2], **and W. A. McKay**[3]

[1]National Centre for Groundwater Research and Training, Adelaide, Australia
[2]University of Bayreuth, Bayreuth, Germany
[3]Desert Research Institute, Reno, Nevada, USA

Received: 1 March 2012 – Accepted: 19 March 2012 – Published: 2 April 2012

Correspondence to: M. Shanafield (mshanafield@yahoo.com)

Published by Copernicus Publications on behalf of the European Geosciences Union.

Abstract

Although many studies examine the use of heat as a tracer to determine vertical infiltration of water into the streambed, few consider the case where both water and heat flow (advection and conduction) are in the upwards direction. In this study, we compare the usefulness of both a one-dimensional numerical model and two analytical solutions for the case where water movement is upwards and the (flat) groundwater temperature is greater than the diel temperatures at the surface. We first create a theoretical test case to compare expected temperature traces at various depths within the sediment column for each model both in the presence and absence of a vertical temperature gradient. These theoretical results are discussed in light of the assumptions inherent in the models. Then the models are applied to a study area located along a reach of the Truckee River in Nevada, USA, during the winter season and flux estimates both between models and between sensor depths are compared. Our results show that despite violation of some assumptions inherent in the analytical models, flux estimates over the entire vertical streambed column can be within one order of magnitude of the numerical model under some conditions. Further, predictions of downwards flux obtained using only the shallow sensors highlight the need to consider the physical processes to be measured when choosing sensor depth, especially when advection and conduction are upwards.

1 Introduction

Heat as a tracer has been used in many studies, with both numerical and analytical approaches, due to the availability of robust and high frequency temperature measurements and the relative simplicity of data analysis (Constantz, 2008). One-dimensional (1-D) and two-dimensional (2-D) models such as VS2DI (Healy and Ronan, 1996) and Hydrus (Simunek et al., 2005) are publicly available and offer comprehensive pre- and post-processing tools. More recently, automated routines for variations on the analytical solutions presented by Bredehoeft and Papadopolus (1965) and Stallman (1965) have also been developed. Arriaga and Leap (2006) describe a simple spreadsheet method of determining fluxes using the Bredehoeft and Papadopolus (1965) solution (BP). Swanson et al. (2011) developed a MATLAB program that allows users to quickly calculate 1-D flux estimates for vertical profiles using the analytical approaches documented in Bredehoeft and Papadopolus (1965), Hatch et al. (2006), Keery et al. (2007), and Schmidt et al. (2007). Gordon et al. (2012) also developed a signal processing routine that allows users to take advantage of high vertical resolution transient temperature data to estimate water fluxes at various depths in the streambed.

However, each methodological approach has inherent assumptions. A key research question is to compare the flux results when the assumptions are violated. One-dimensional, analytical solutions are not appropriate for all spatial geometries and under all boundary conditions. Lautz (2010) examined the limitations imposed on the use of the Stallman solution when each of its three key boundary conditions are violated. Shanafield et al. (2011) further investigated the limitations of the Stallman solution when uncertainty in sediment thermal properties exists. Both Stallman (1965) and Silliman et al. (1995) designated lower limits on the application of the Stallman solution as flux goes to zero. Bredehoeft and Papadopolus (1965) also discussed a minimum detectable velocity for the analytical solution they present, and Schmidt et al. (2006) and Anibas et al. (2009) showed that BP is not applicable for transition periods, when small inverse temperature gradients result in the estimation of upward flow.

We examine the case where groundwater temperature is higher than surface water temperature and the total head of the stream is less than the streambed potentiometric head (i.e. a gaining stream). For this case, advection and conduction processes are directed upward from the streambed to the river. Using hypothetical boundary conditions and vertical infiltration velocity, we use a simple numerical model as well as two analytical solutions, BP and the Hatch et al. (2006) or Keery et al. (2007) formulation of the Stallman solution (HK), to predict the transient vertical temperature distributions at depths to 1 m below the streambed. The results are compared for the case where

HESSD
9, 4305–4332, 2012

advection and conduction are both upward, and where there is no temperature gradient with depth. We then use the same models to estimate vertical infiltration velocities for a nine-day period during January 2007 in a gaining river with surface temperatures greater than the observed groundwater temperatures in the streambed. Our objective is to understand the following:

- Can we use the BP and HK analytical solutions when both streambed convection and conduction are upward?
- How do results from each of these analytical models compare to the numerical estimates under these conditions?
- How important are the sampling depths under these conditions?

Previous studies have compared numerical models to the Stallman analytical solution (Hatch et al., 2006; Lautz, 2010) or to the Bredehoeft and Papadopolus model (Anibas et al., 2009). However, to our knowledge, previous studies have not compared the performance of both HK and BP with a numerical model under upward flux field conditions.

2 Hypothetical simulation using numerical and analytical models

2.1 Numerical model

Under homogeneous and isotropic conditions in a saturated column, the 1-D heat and fluid flow equation can be written as

$$\frac{K}{\rho c}\frac{\partial^2 T}{\partial z^2} - \frac{\rho_w c_w q_z}{\rho c}\frac{\partial T}{\partial z} = \frac{\partial T}{\partial t} \quad (1)$$

where, T is the temperature at time t and depth z, c_w is specific heat of the fluid, ρ_w is density of the fluid, c is the specific heat of the saturated media, ρ is the density of saturated media, K is thermal conductivity of saturated media (assuming negligible dispersion), and q_z is vertical Darcy velocity (a flux). In this study, positive q_z values always denote upwards water flux. For the hypothetical simulation, the Darcy velocity was set to $0.25\,\mathrm{m\,d^{-1}}$ (i.e. upwards flow of water), and the streambed properties typical of a porous medium similar to sand were selected (Table 1). Temperature at the upper boundary condition (T_o) was varied diurnally using the equation:

$$T_o = T_{\text{avg}} + A\sin(2\pi t/P) \tag{2}$$

where P is the period of oscillation (1 day), A is the amplitude of oscillation during P (±2 °C), T_{avg} is the average temperature over P (3 °C), and t is the time (days). The lower temperature boundary condition was set to a constant 10 °C to simulate upwards convection, and to 3 °C to produce no mean temperature gradient with depth. The model was assigned a total depth of 1 m, with nodes every 0.02 m and temperatures were output at the nodes located at depths of 0.05, 0.10, 0.20, 0.30, 0.40, and 0.50 m and run to steady state for both lower boundary condition scenarios (Fig. 1a and d).

2.2 BP

The Bredehoeft and Papadopolus (1965) solution to Stallman's (1960) general equation, for the case of steady-state vertical flow of both groundwater and heat through a semi-confining layer is given as:

$$\frac{(T_z - T_o)}{(T_L - T_o)} = \left[\frac{\exp\left(^{\beta z}/_{L}\right) - 1}{\exp(\beta) - 1}\right] \tag{3}$$

where, T_z is temperature at the depth of interest z, T_o is the uppermost temperature measurement, T_L is the lower temperature measurement, L is the total vertical distance between T_o and T_L, $\beta = c_\mathrm{w}\rho_\mathrm{w}v_zL/K$, and v_z is the fluid velocity. As written, positive

HESSD
9, 4305–4332, 2012

fluxes indicate downward flow ($v_z = -q_z$). Bredehoeft and Papadopolus developed a set of type curves to estimate groundwater flux based on Eq. (3).

The BP method assumes steady, uniform, one-dimensional, vertical, isotropic, anisothermal flow of an incompressible fluid through a homogeneous, fully saturated semiconfining layer. Implicitly, fluid flow can be either upward or downward and temperature must be in the same direction or the sign on the left side of Eq. (3) is the opposite of the right and Eq. (3) is invalid. The magnitude of v_z that is detectable using the BP method is dependent on the sediment thermal properties and L. Given the thermal properties used in this study (Table 1) and an L of 1 m, the least magnitude of v_z would be 0.2 m d^{-1}. Additionally, for small inverse temperature gradients, negative flux or upward flow is estimated independent of hydraulic gradients, suggesting that this solution is of limited applicability during e.g. fall and spring transition periods, as suggested by Schmidt et al. (2006) and Anibas et al. (2009).

Similar to the numerical model, L was assigned as 1 m, q_z was set to 0.25 m d^{-1}, the sediment properties were assigned from Table 1, and T_z was computed at depths of 0.05, 0.10, 0.20, 0.30, 0.40, and 0.50 m (Fig. 1b and e).

2.3 HK

When dispersivity is neglected, the Hatch et al. (2006) and Keery et al. (2007) methods of solving the Stallman equation yield identical results. This equation can be written as (Hatch et al., 2006):

$$T_z(z,t) = A\exp\left(\frac{v_f z}{2K_e} - \frac{z}{2K_e}\sqrt{\frac{\alpha + v_f^2}{2}}\right)\cos\left(\frac{2\pi t}{P} - \frac{z}{2K_e}\sqrt{\frac{\alpha - v_f^2}{2}}\right) \quad (4)$$

where K_e is effective thermal diffusivity of the saturated sediment, v_f is the thermal front velocity given as $v_f = q_z \frac{c_w \rho_w}{c\rho}$ and $\alpha = \sqrt{v_f^4 + (8\pi \cdot K_e/P)^2}$.

HESSD
9, 4305–4332, 2012

The Stallman (1965) analytical solution assumes nonsteady, uniform, one-dimensional, vertical, anisothermal flow of an incompressible fluid through homogeneous, fully saturated porous media. The upper boundary surface temperature varies with constant amplitude, harmonically over time. Furthermore, Stallman tacitly implies that constant amplitude temperature fluctuations at all depths decrease to the mean of the temperature fluctuations at the land surface, including the constant groundwater temperature at the lower boundary condition; therefore, no mean temperature gradient with depth. In Stallman's description, it is further implied that fluid flow is downward and positive for infiltration; however, Stallman (1965) does not specifically state that water and heat flow *must* be in the same direction. Utilizing natural media with average heat properties, Stallman found that this solution could be used to predict infiltration into the subsurface at rates as low as $0.003\,\mathrm{m\,d^{-1}}$, whereas Silliman et al. (1995) suggested $0.007\,\mathrm{m\,d^{-1}}$ as the minimum fluid velocity.

Because they are derived from the Stallman (1965) solution, the same assumptions are true for both the Hatch et al. (2006) and Keery et al. (2007) methods. Both of these authors apply their methods to upwards, as well as downwards water flow, the former theoretically, and the latter using field data. Following Hatch et al. (2006), the amplitude ratio is most sensitive to low downward flow, especially as probe spacing increases. However, for a probe spacing of 0.05–0.5 m, as used in the current study, a Darcy velocity of $0.25\,\mathrm{m\,d^{-1}}$ (upwards) should be well within the limits of sensitivity. However, Shanafield et al. (2011) showed that the application of the Stallman analytical solution is limited for upward fluxes, especially where the lower sensor reports a flat temperature signal.

For the hypothetical test case, Eq. (4) was used to create temperature traces at depths (z) of 0.05, 0.10, 0.20, 0.30, 0.40, and 0.50 m (Fig. 1c and f). As in the other models, A was 2 °C, q_z was set to $0.25\,\mathrm{m\,d^{-1}}$, sediment properties were assigned from Table 1, and P was 1 day.

HESSD
9, 4305–4332, 2012

2.4 Results

With a lower temperature boundary condition of constant 10 °C, comparison of the BP simulations with the numerical solution (over a 24-h period) yielded RMSE values decreasing from 0.60 °C at a depth of 0.05 m to 0.05 °C at a depth of 0.5 m. When the lower temperature boundary was decreased to 3 °C so that there was no mean vertical temperature gradient in the column, the 0.5 m depth BP RMSE was slightly lower at 0.49 °C, while the values at the other depths did not change from the previous simulation. For both simulations, the highest RMSE value was estimated at a depth of 0.10 m (RMSE = 0.64 °C for both boundary conditions). At this depth, the numerical method shows a sinusoidal diurnal signal which is attenuated and lagged compared to the boundary condition. The BP method, because it is a steady state solution, does not capture that phase shift. Due to the assigned upwards advection of water (and conduction as well for the 10 °C lower boundary condition) and the thermal properties of the sediment, this diel change in temperature is less than 0.01 °C at a depth of 0.2 m and essentially 0 °C below that. Therefore the lack of phase shift in the BP solution at these depths is not a source of error.

When the lower boundary condition was set to 10 °C, the HK simulations had RMSE values increasing from 1.11 °C at a depth of 0.05 m to 6.76 °C at a depth of 0.5 m. Because HK does not have a lower temperature boundary condition, at a depth of 0.5 m the error using this method was three times the amplitude of the diurnal signal at the top. The presence of the vertical temperature gradient greatly affected how accurately the HK model matched numerical temperature traces, especially at depth. This is because Eq. (4) describes temperature in the "top half-space" and does not use the lower temperature boundary condition. Therefore it cannot account for upward convection. Theoretically, the higher temperature at the lower boundary condition could be used for the upper boundary condition to drive the convective flux; however, there is no sinusoidal signal in that lower boundary condition, which violates another of the assumptions inherent in the method.

When the mean vertical temperature gradient was removed, the HK RMSE values improved, decreasing from 1.00 °C at a depth of 0.05 m to 0.001 °C at a depth of 0.5 m. Visual comparison of Fig. 1d and e shows good agreement between the numerical and HK methods, with attenuation of the diel signal at depth occurring more slowly for HK than the numerical method, but faster with BP.

3 Field example

3.1 Field methods

Temperature and stream stage data were collected at the downstream end of a pointbar within the lower Truckee River, located in an arid region 27 km east of Reno, Nevada on the eastern slope of the Sierra Nevada Mountains. The streambed sediments at this location are primarily composed of alluvial deposits of mixed cobble, gravel, and sand to a depth of at least 10 m (Shope, 2009). The sediment grain size distribution was identified as predominately medium sand to medium gravel (0.5–15 mm) and cobbles (15–65 mm).

A 0.025 m diameter, PVC piezometer was installed in the streambed to a depth of 0.390 m with a screened interval over the bottom 0.051 m. A stainless steel cable was suspended inside the piezometer and DS1921Z I-Button Dataloggers (−5 °C to 26 °C, ±0.5 °C, Dallas Semiconductor Maxim, Sunnyvale CA) were suspended from the cable at depths of 0.040, 0.210, and 0.375 m below the streambed surface. No aggradation or degradation was observed during the field study period. Prior to field deployment, dataloggers were placed into a circulation bath (NESLAB RTE 17, Thermo, Portsmouth, NH) and the recorded datalogger temperatures within the expected field interval were compared to an ASTM NIST certified precision thermometer accurate to 0.1 °C. Transient temperature variations between dataloggers equilibrated within 15 min and a second order polynomial regression was used to estimate nonlinear temperature variations. This methodology increased the precision of the dataloggers from

HESSD
9, 4305–4332, 2012

the manufacturer suggested 0.5 °C uncertainty to less than 0.2 °C. Differences between the observed and calibrated temperatures averaged 0.1 °C with maximum deviations of 0.2 °C. Stream water elevation was monitored with a TruTrack water height and temperature datalogger (Tru Track Ltd, Christchurch, NZ). A 9-day period of hourly temperature and stream stage measurements from 17 to 26 January 2008 was selected for analysis (Fig. 2).

Although stream stage and the piezometric elevation were not concurrently measured during this study, previous 1-D hydraulic, 1-D heat based, and 3-D flow and transport estimates indicate vertical upward flux dominates at this location (Fig. 3 and Shope et al., 2012; Shope, 2009). Surface water discharge during this period was $10.60 \pm 0.38\,\mathrm{m^3\,s^{-1}}$, indicating that surface water discharge varied less than 4 % throughout the study period and that steady state head conditions could be assumed.

Throughout the study period, near-surface temperatures were typically cooler than subsequently deeper temperatures. In 11 of the 216 timesteps (5 %), the 0.040 m depth was cooler than the surface temperature. In this case, fluid flow was upward while heat conduction was downward resulting in the left hand side of Eq. (3) becoming negative. The assumption that heat and fluid flow are in the same direction is violated and thus, Eq. (3) is invalid. Therefore, we adjusted the data so that surface temperatures over the entire study period were cooler than the temperatures at 0.040 m. Hydraulic conductivity was estimated with falling head tests, and other streambed thermal and hydraulic parameters representative of medium sand to gravel were selected (Table 1).

3.2 Modeling

3.2.1 Numerical model

A 1-D, numerical estimate of vertical flux was obtained with Hydrus 1-D (Simunek et al., 2005). Hydrus 1-D numerically solves Eq. (1). The streambed thermal and hydraulic parameters were the same as for the hypothetical model, because the dominant observed sediment type was medium sand to gravel (Table 1). The parameters

HESSD
9, 4305–4332, 2012

were consistent with measured streambed sediment properties, which remained constant with depth and were obtained from the literature. The upper boundary conditions were measured temperatures at the streambed interface and stream stage. Measured temperatures and an initially estimated time-variable flux were assigned to the lower boundary (Fig. 4).

The temperatures and head consistent with the first timestep were assigned as initial conditions throughout the model domain. The model was subsequently run until steady-state conditions were obtained. The vertical flux at the depth of the lowest thermistor (lower boundary) was then inversely solved at each timestep by optimizing the observed and simulated temperature at intermediate depths, both manually and with the automated PEST parameter optimization routine (Doherty, 2004).

Water flux through the model was estimated by optimizing the fit between simulated and observed temperatures at the 0.040 m and 0.210 m datalogger depths assuming either a constant flux over the entire 9-day time period (Fig. 5a) or a time-variable flux optimizing the residual at each one-hour timestep (Fig. 5b). The best fit for constant flux was 0.36 m d^{-1}, with RMSE values of 0.46 °C and 0.31 °C for the 0.040 and 0.210 m depths, respectively. Using time-variable flux for the lower boundary condition, a better fit with measured data at 0.210 m was achieved, with a flux of 0.48 ± 0.08 m d^{-1} and RMSE values of 0.56 °C and 0.10 °C for the 0.040 and 0.210 m depths, respectively. The assumption of constant flux at the upper boundary had slightly better fit to the data at the 0.04 m depth than when the upper boundary was a time-variable flux; however, the 0.21 m depth had the opposite result. The simulated temperatures using constant flux were both higher and lower in amplitude than the fit with time-variable flux. Temperature data from 22 through 24 January was difficult to accurately simulate with either a constant or a time-variable flux at the lower boundary. When this period is neglected, the fit at 0.040 m is better using the time-variable flux, as would be expected. The results of this numerical approach were compared to Darcy velocity estimates from each of the analytical solutions (Fig. 6, Table 2).

HESSD
9, 4305–4332, 2012

3.2.2 BP

The BP flux was estimated by adjusting the β term and explicitly minimizing the difference between each side of Eq. (3). The Bredehoeft and Papadapolus method requires temperatures from three depths; therefore, four possible combinations of the available temperature data were possible. The first two were calculated using the surface water (SW) and 0.375 m temperatures as boundaries with 0.040 m as an intermediate temperature (BP1) and the same boundaries with the 0.210 m temperatures as an intermediate temperature (BP2). For BP3, the 0.040 m and 0.375 m temperatures were the boundaries, with the 0.210 m as an intermediate temperature. For BP4, the SW and 0.210 m temperatures were the boundaries, with 0.040 m as the intermediate temperature.

In general, the BP results agreed closely with numerical results; average estimated q_z values for BP2 and BP3 were 0.24 and 0.17 m d^{-1}, respectively (Fig. 6b, Table 2). Mean differences in fluxes between Hydrus and BP3 was 0.01 °C and even less for BP2. The BP1 and BP4 estimated fluxes were more variable, with higher averages of 0.38 and 0.45 m d^{-1}, respectively (Fig. 6b, Table 2). When the total depth (L) was reduced, q_z increased (i.e. strongly upwelling) by decreasing the right hand side of Eq. (3).

3.2.3 HK

Both daily and hourly q_z estimates were calculated using the HK method. The daily estimates were manually calculated using unfiltered data. First, the daily amplitude of observed temperature was manually selected for each depth. Next, the amplitude ratios A_r between paired thermistors were calculated by dividing the amplitude of the daily temperature signal at the deeper sensor (A_d) by that of the shallow sensor (A_s), where $A_r = A_d/A_s$. Sediment properties were selected from Table 1. The thermal front velocity (v_f) was then iteratively calculated using the equation (Hatch et al., 2006):

$$v_f = \left(\frac{2K_e}{\Delta z} \ln A_r + \sqrt{\frac{\alpha + v_f^2}{2}} \right) \tag{5}$$

and q_z was calculated from v_f using $q_z = v_f \frac{c\rho}{c_w \rho_w}$.

Equation (5) requires temperatures at only two depths to estimate fluid flux, rather than at three depths required for the BP estimates. These temperatures must show a diel trend; i.e. it must be possible to discern a clear sinusoidal signal in both temperature traces. The thermal front velocity also can be determined from the Stallman solution using the shift in time between peak temperatures observed at depth within the sediment. However, this phase shift method was not used in the current study for several reasons: (1) measured temperatures did not consistently show a clear shift in peak temperatures at depth, (2) the amplitude ratio method is more reliable in non-ideal conditions (Lautz, 2010) such as for the temperature gradient present in the current study, (3) the phase shift method cannot determine the direction of flow, and (4) most of the existing literature using the HK method focuses on the amplitude ratio method, making this method more useful for comparison.

Because there is no diel trend, the 0.375 m data was not usable for determining daily q_z with the HK method. Three temperature combinations were suitable for analysis; surface water to 0.040 m (S1), surface water to 0.210 m (S2), and 0.040 m to 0.210 m (S3). Amplitude ratios using hand-picked daily maxima and minima were between 0.07 and 0.60 (average amplitude ratio was 0.35, 0.15, and 0.36 for S1, S2, and S3, respectively), showing that the sensor spacing was appropriate for this method. S1 and S2 both estimated predominantly downward Darcy velocity (average q_z of 0.98 and 0.09 m d^{-1}, respectively). Fluxes predicted by S3 were generally upwards and within 25 % of the numerical estimate, with an average of 0.18 m d^{-1} (Table 2 and Fig. 6b). Because the observed temperatures at 0.040 m and 0.210 m each had the same amplitude on 22 January, the S3 flux estimate for that day was not determined.

Discussion Paper | Discussion Paper | Discussion Paper | Discussion Paper |

HESSD

9, 4305–4332, 2012

Estimation of upward flux through streambed sediments

M. Shanafield et al.

By filtering field data to extract only the diel signal, it becomes possible to estimate infiltration velocity not only over a full diel period, but at many smaller timesteps within that period. Hourly HK estimates were determined using the program VFLUX, a set of MATLAB routines designed to estimate vertical flux through pairs of sensors on a single profile (Gordon et al., 2012). The diel signal is isolated from each temperature trace using Dynamic Harmonic Regression (Keery et al., 2007), which then allows calculation of q_z at hourly timesteps using Eq. (5). For comparison with the daily HK results, the same combinations of sensors were used with VFLUX: SW to 0.040 m (V1), SW to 0.210 m (V2), 0.040 m to 0.210 m (V3). This method also allowed q_z to be calculated using two additional intervals: SW to 0.375 m (V4, as in BP1 and BP2) and 0.210 m to 0.375 m (V5). Amplitude ratios computed by the VFLUX program were between 0.02 and 0.53, similar to the daily amplitude ratios. After being filtered, the essentially flat temperature signal recorded at the 0.375 m resulted in a constant amplitude of 0.02 °C over the entire study period.

The results from this filtered HK approach were generally closer to the numerical method estimates (Table 2 and Fig. 6c). V2, V4, and V5 all predicted upward water movement, with average q_z values within 9 %, 29 %, and 50 % of the numerical estimate, respectively. Contrary to S1, V1 estimated high upward Darcy velocity, whereas the opposite was true for V3. Thus, unlike the daily HK estimate, there is no trend between q_z and the magnitude of the combined depth of the sensors. It is recommended that the first and last 2–3 days of data be discarded after the data has been filtered (Gordon et al., 2012); however, in this case only 3 days of data would remain. Further, estimates at the beginning and end did not deviate significantly from the remaining data. Therefore, this data was not removed from the results.

4 Discussion and conclusions

Although many recent studies using heat as a tracer focus on fieldsites in which advection and conduction are downwards into the sediment, few have considered the case

HESSD
9, 4305–4332, 2012

of upwards advection and conduction. In their original applications, both the BP and Stallman (1965) analytical methods were presented with downwards flux examples. This study highlights the differences between the BP and HK methods and the numerical solution to the heat transport equation under conditions of upward advection and conduction. Each of these models is subject to the limitations imposed by its inherent assumptions. For a given infiltration velocity and sediment properties, the expected diel variation in temperatures at various depths was modeled. Given this set of parameters, when the groundwater temperature was 10 °C, the numerical method predicted only a minimal diel variation in temperature at a depth of 0.20 m, and essentially flat, but higher temperatures at greater depths into the streambed. Average temperatures at depth were closely reproduced by the BP method, although this solution predicted a diel signal propagating to 0.50 m. Conversely, the HK method also predicted the attenuation of the temperature signal below 0.20 m, but could not capture the gradient in temperatures caused by the advection and conduction of warmer water from the subsurface.

Estimated sediment thermal properties for the field data were the same as for the theoretical exercise, allowing analysis of the effects of boundary conditions and assumptions in the analytical equations on the predicted Darcy velocities obtained with the BP and HK methods. Although numerical models require additional information beyond what is needed for the analytical solutions (i.e. hydraulic conductivity and head or flux boundary conditions), they are not bound by the restrictive assumptions necessary for analytical solutions and may better represent field conditions. For the Hydrus model, the availability of temperature data at two intermediate depths and time-variable hydraulic head at the surface was useful. Unlike most areas of even moderate downward flux, the temperature signal even at the shallow depth of 0.375 m at the bottom boundary was flat, whereas temperatures at the upper boundary in the surface water were not necessarily controlled by water movement in the sediment column. Therefore, temperatures at intermediate depths in the sediment column provided necessary information on heat transport and water flux through the sediments.

HESSD
9, 4305–4332, 2012

The numerical model presents a well-constrained estimate of flux through the entire 1-D column between the surface water and 0.375 m sensor. Using a variable flux boundary condition, the best numerical model was able to fit data at 0.210 m with a low RMSE of 0.10 °C. Possible sources of error between measured and simulated temperatures include the influence of non-vertical hyporheic flow (especially for the top sensors) and uncertainty or vertical variability in thermal or hydraulic conductivity values. A sensitivity analysis of these parameters is outside the scope of the current study. However, similar to the results of the numerical model during the theoretical exercise at the same infiltration velocity, the field data showed a diurnal signal at 0.210 m, and essentially a flat temperature at a depth of 0.375 m. These results, along with the low RMSE value of 0.10 °C, suggest that the sediment thermal properties and hydraulic conductivity used in the model for the field data are reasonable.

Although BP is a steady-state solution and, as demonstrated by the theoretical exercise, the method does not capture time lags in the arrival of the thermal signal at depth, it is appropriate for the estimation of infiltration velocity when advection and conduction are upwards. BP produced flux estimates that had a low error when compared to the numerical model. Of all the HK models, V2 had the lowest error in comparison to the numerical model. Filtering of the data separates the diel temperature signal from trends and white noise in the signal caused by seasonal and localized weather changes. This data processing step eliminates potential difficulties in calculating the amplitude that may be caused by local maxima or minima within a daily period or inaccuracies in the amplitude at a certain sensor caused by steep or abrupt changes in temperature trends over time. Some trends and noise were present in the Truckee River field data (Fig. 2), limiting comparison of the VFLUX results with daily estimates. Given the theoretical results showing the error that results when the bottom boundary condition is not taken into account under these conditions, the correct prediction of flux direction in one of the daily HK models and several of the filtered models was unexpected.

The 1-D analysis of streambed flux is subject to many limitations and not appropriate for all natural conditions; however, estimation of local vertical fluxes based on temperature attenuation remains a common method of determining streambed exchange (Constantz, 2008). Additional 1-D methods are found in the literature, but were not included in the comparison because they were not appropriate for the conditions encountered at this site. For example, temperature envelopes have been used to determine vertical flux of water through the streambed on a seasonal scale (Bartolino and Niswonger, 1999). Turcotte and Schubert (1982) also formulated a version of the analytical equation; however, it is restricted to upward flow and not selected for this study because of this limited application. Finally, Izbecki and Michel (2002) applied a one-dimensional heat loss equation to determine infiltration during winter months in an intermittent stream. However the seasonal method that they used was not explicitly designed and tested for fully saturated medium or for the hourly and daily timesteps selected in the current study.

As indicated by this study, 1-D estimates are not all equal, and it is important to consider the assumptions and limitations inherent in each of these methods. Despite transgression of some assumptions in both the BP and HK methods, certain combinations of sensors produced flux estimates similar to the numerical method. Because fluid and heat flow was driven from the bottom in this study, the estimated fluxes over various combinations of sensor depths was extremely variable. Very shallow temperatures often show the combined effects of hyporheic flow, solar radiation, and it can be difficult to separate the effects of these factors from interactions with underlying groundwater. These results highlight the need for consideration of sensor spacing and selection in determining flux through streambed sediments, because shallow sensor selection can lead to flux estimates describing different physical streambed processes than would be captured by a longer sediment column.

Acknowledgements. The authors would like to thank David E. Prudic (University of Nevada, Reno) for his helpful advice and suggestions on the manuscript, and Greg Pohll (Desert Research Institute, Reno, Nev.) for sharing his numerical heat transport code. Field study funding was provided through the USEPA Office of Research and Development, Landscape Ecology Branch Initiative. Support for the first and second authors from the National Center for Groundwater Research and Training (NCGRT) at Flinders University and from the Interdisciplinary

HESSD
9, 4305–4332, 2012

Research Project TERRECO funded by the German Research Foundation (DFG) at the University of Bayreuth is greatly acknowledged.

References

Anibas, C., Fleckenstein, J. H., Volze, N., Buis, K., Verhoeven, R., Meire, P., and Batelaan, O.: Transient or steady-state? Using vertical temperature profiles to quantify groundwater-surface water exchange, Hydrol. Process., 23, 2165–2177, 2009.

Arriaga, M. A. and Leap, D. I.: Using solver to determine vertical groundwater velocities by temperature variations, Purdue University, Indiana, USA, Hydrogeol. J., 14, 253–263, doi:10.1007/s10040-004-0381-x, 2006.

Bartolino, J. R. and Niswonger, R. G.: Numerical Simulation of Vertical Ground-Water Flux of the Rio Grande from Ground-Water Temperature Profiles, Central New Mexico, United States Geological Survey, Albuquerque, NM99-4212, 40, 1999.

Bredehoeft, J. D. and Papadopulos, I. S.: Rates of Vertical Groundwater Movement Estimated from the Earth's Thermal Profile, Water Resour. Res., 1, 325–328, 1965.

Carsel, R. F. and Parrish, R. S.: Developing joint probability distributions of soil water retention characteristics, Water Resour. Res., 24, 755–769, 1988.

Constantz, J.: Heat as a tracer to determine streambed water exchanges, Water Resour. Res., 44, W00D10, doi:10.1029/2008WR006996, 2008.

Constantz, J. and Stonestrom, D. A.: Heat as a tool for studying ground-water movement near streams, in: Heat as a tool for studying the movement of ground water near streams, edited by: Constantz, J. and Stronestrom, D. A., United States Geological Survey Circular 1260, 1–6, 2003.

Doherty, J.: PEST, Model-Independent Parameter Estimation User Manual: Fifth Edition, Watermark Numerical Computing, 300, 2004.

Gordon, R. P., Lautz, L. K., Briggs, M. A., and McKenzie, J. M.: Automated calculation of vertical pore-water flux from field temperature time series using the VFLUX method and computer program, J. Hydrol., 420–421, doi:10.1016/j.jhydrol.2011.11.053, 2012.

Hatch, C. E., Fisher, A. T., Revenaugh, J. S., Constantz, J., and Ruehl, C.: Quantifying surface water-groundwater interactions using time series analysis of streambed thermal records:

Method development, Water Resour. Res., 42, W10410, doi:10410.11029/12005WR004787, 2006.
Healy, R. W. and Ronan, A. D.: Documentation of Computer Program VS2DH for Simulation of Energy Transport in Variably Saturated Porous Media. Modification of the U. S. Geological Survey's Computer Program VS2DT, United States Geological Survey, Denver, Colorado.Water Resources Investigations Report 96-4230, 1996.
Ingebritsen, S. E. and Sanford, W. E.: Groundwater in Geologic Processes, Cambridge Univ. Press, New York, 1998.
Izbicki, J. A. and Michel, R. L.: Use of Temperature Data to Estimate Infiltration from Intermittent Streams in the Western Mojave Desert, USA, in: Balancing the Ground Water Budget, edited by: Foo, D. Y., Proceedings of the International Association of Hydrogeologists, 12–14 May 2002, 1 CD-ROM, Darwin, Australia, 2002.
Keery, J., Binley, A., Crook, N., and Smith, J. W. N.: Temporal and spatial variability of groundwater-surface water fluxes: Development and application of an analytical method using temperature time series, J. Hydrol., 336, 1–16, 2007.
Lapham, W. W.: Use of temperature profiles benath streams to determine rates of vertical ground-water flow and vertical hydraulic conductivity, United States Geological Survey Water Supply Paper 2337, 1989.
Lautz, L. K.: Impacts of nonideal field conditions on vertical water velocity estimates from streambed temperature time series, Water Resour. Res., 46, W01509, doi:10.1029/2009wr007917, 2010.
Niswonger, R. and Prudic, D. E.: Modeling heat as a tracer to estimate streambed seepage and hydraulic conductivity, in: Heat as a tool for studying the movement of ground water near streams, edited by: Constantz, J. and Stronestrom, D. A., United States Geological Survey Circular 1260, 81–89, 2003.
Schmidt, C., Bayer-Raich, M., and Schirmer, M.: Characterization of spatial heterogeneity of groundwater-stream water interactions using multiple depth streambed temperature measurements at the reach scale, Hydrol. Earth Syst. Sci., 10, 849–859, doi:10.5194/hess-10-849-2006, 2006.
Schmidt, C., Conant, B., Bayer-Raich, M., and Schirmer, M.: Evaluation and field- scale application of an analytical method to quantify groundwater discharge using mapped streambed temperatures, J. Hydrol., 347, 292–307, doi:10.1016/j.jhydrol.2007.08.022, 2007.

Shanafield, M., Hatch, C., and Pohll, G.: Uncertainty in thermal time series analysis estimates of streambed water flux, Water Resour. Res., 47, W03504, doi:10.1029/2010wr009574, 2011.
Shope, C. L.: Water and Heat Fluxes in a Channel Bar Compared with Adjacent Streambed and Streambank Hydrogeology, Program of Hydrologic Sciences, University of Nevada, Reno, NV, 226 pp., 2009.
Silliman, S. E., Ramirez, J., and McCabe, R. L.: Quantifiying Downflow Through Creek Sediments Using Temperature Time Series: One-Dimensional Solution Incorporating Measured Surface Temperature, J. Hydrol., 167, 99–119, 1995.
Simunek, J., Genuchten, M. T. v., and Sejna, M.: The HYDRUS-1D Software Package for Simulating the One-Dimensional Movement of Water, Heat, and Multiple Solutes in Variably-Saturated Media – Version 3.0, Dep. of Environ. Sci., Univ. of Calif., Riverside, Calif., 240 2005.
Stallman, R. W.: Notes on the Use of Temperature Data for Computing Ground-Water Velocity (also in Methods of Collecting and Interpreting Ground-Water Data, compiled by Bentall, R., 1963, U.S. Geol. Survey. Water Supply Paper 1544-H, 36–46, 1963), 6th Assembly on Hydraulics, Nancy, France, 1–7, 1960.
Stallman, R. W.: Steady One-Dimensional Fluid Flow in a Semi-Infinite Porous Medium with Sinusoidal Surface Temperature, J. Geophys. Res., 70, 2821–2827, 1965.
Swanson, T. E. and Cardenas, M. B.: Ex-stream: a MATLAB program for calculating fluid flux through sediment-water interfaces based on steady and transient temperature profiles, Comput. Geosci., 37, 1664–1669, 2010.
Turcotte, D. L. and Schubert, G.: Geodynamics: Applications of Continuum Physics to Geological Problems, John Wiley & Sons, New York, 1982.

HESSD
9, 4305–4332, 2012

Estimation of upward flux through streambed sediments

M. Shanafield et al.

Table 1. Hydraulic and thermal sediment properties used for numerical and analytical modeling.

Study area physical properties and boundary conditions			
Parameter	Description	Value	Unit
n (sand)	Porosity	0.4	
K_s	Saturated hydraulic conductivity	1.95	$m\ d^{-1}$
c_w	Specific heat of water	4186	$J\ kg^{-1}\ °C^{-1}$
ρ_w	Density of water	1000	$kg\ m^{-3}$
c	Specific heat of the saturated sediment	1910[a]	$J\ kg^{-1}\ °C^{-1}$
ρ	Density of the saturated sediment	1800[b]	$kg\ m^{-3}$
K	Saturated thermal conductivity	1.8[c]	$W\ m^{-1}\ °C^{-1}$
K_e	Effective thermal diffusivity	0.0452[d]	$m^2\ d^{-1}$
α	Van-Genuchten alpha	0.0145[e]	
n_{VG}	Van-Genuchten n	0.0268[e]	m^{-1}
m_{VG}	Van-Genuchten m	0.627	

[a] Constantz and Stonestrom (2003); [b] Lapham (1989); [c] Midpoint of range from Niswonger and Prudic (2003); [d] $K_e = K/\rho c$ when dispersivity neglected (Ingebritsen and Sanford, 1998); [e] Carsel and Parrish (1988).

HESSD

9, 4305–4332, 2012

Estimation of upward flux through streambed sediments

M. Shanafield et al.

Discussion Paper | Discussion Paper | Discussion Paper | Discussion Paper |

Title Page
Abstract Introduction
Conclusions References
Tables Figures
Back Close
Full Screen / Esc
Printer-friendly Version
Interactive Discussion

Table 2. Average, maximum, and minimum estimated Darcy velocity through the streambed sediment using numerical and analytical heat tracer models (SW denotes observed surface water temperatures). Positive values indicate upwards flow.

Method		Time-step	Boundary conditions	Observ. depth(s)	Avg ($m\,d^{-1}$)	Max ($m\,d^{-1}$)	Min ($m\,d^{-1}$)
Numerical, constant flux		9 day avg.	SW, 0375 m	0.040 m, 0.210 m	0.36	n/a	n/a
Numerical, time-variable flux		Hourly			0.24	0.57	0.04
BP	BP1	Hourly	SW,	0.040 m,	0.38	0.75	0.23
	BP2		0.375 m	0.210 m	0.24	0.46	0.04
	BP3		0.040 m, 0.375 m	0.210 m	0.17	0.37	0.04
	BP4		SW, 0.210 m	0.040 m	0.45	0.99	−0.51
HK	S1	Daily	SW, 0.040 m	n/a	−0.98	−0.29	−1.66
	S2		SW, 0.210 m	n/a	−0.09	0.22	−0.35
	S3		0.040 m, 0.210 m	n/a	0.18	0.38	−0.15
	V1	Hourly	SW, 0.040 m	n/a	1.69	2.32	1.01
	V2		SW, 0.210 m	n/a	0.22	0.40	0.04
	V3		0.040 m, 0.210 m	n/a	−0.28	0.02	−0.70
	V4		SW, 0.375 m	n/a	0.17	0.35	0.05
	V5		0.210 m 0.375 m	n/a	0.12	0.29	−0.07

HESSD
9, 4305–4332, 2012

M. Shanafield et al.

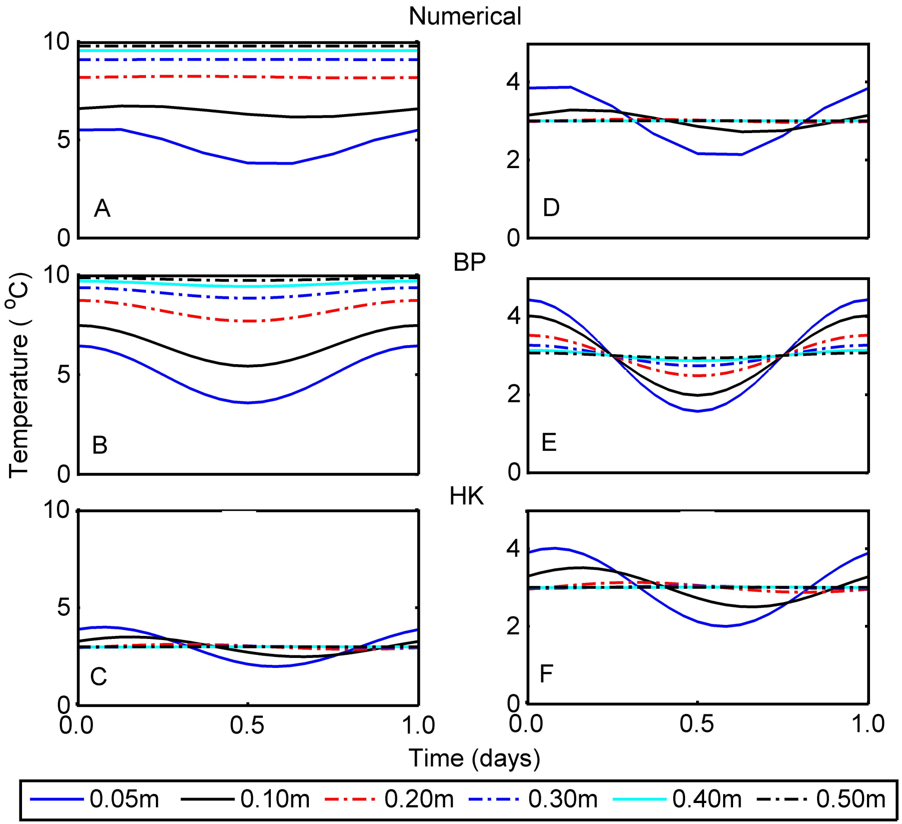

Fig. 1. Comparison of numerical, BP, and HK models when the lower boundary condition is constant at 10 °C **(A–C)** and 3 °C **(D–F)**.

HESSD
9, 4305–4332, 2012

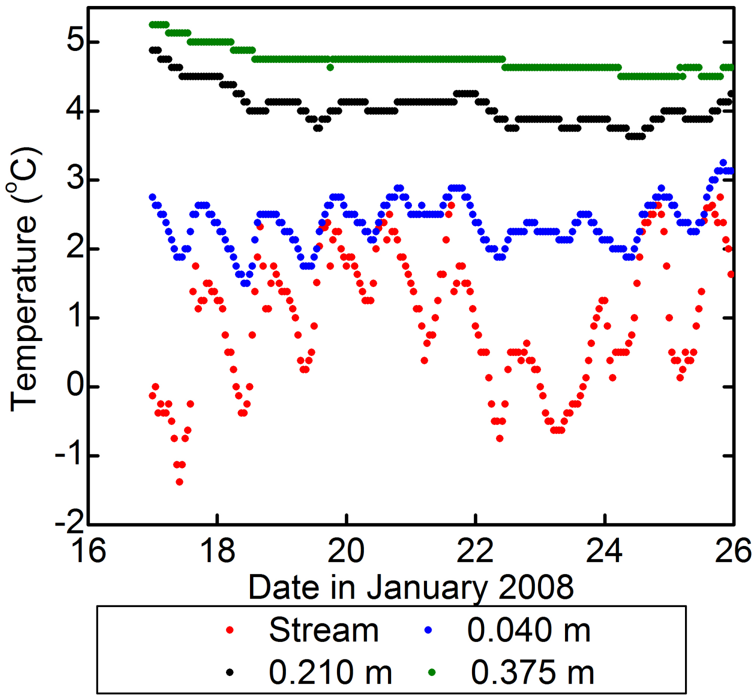

Fig. 2. Temperature data from winter 2008 selected for modeling. Each location is referenced to depth below the streambed.

HESSD
9, 4305–4332, 2012

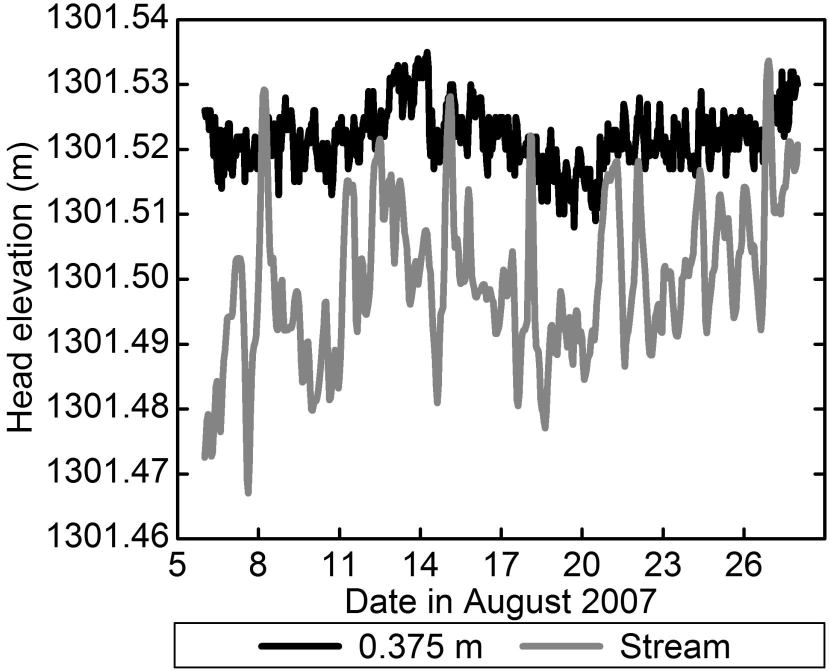

Fig. 3. 2007 data collected at the location of the vertical temperature sensors showing that water movement is generally upwards.

HESSD
9, 4305–4332, 2012

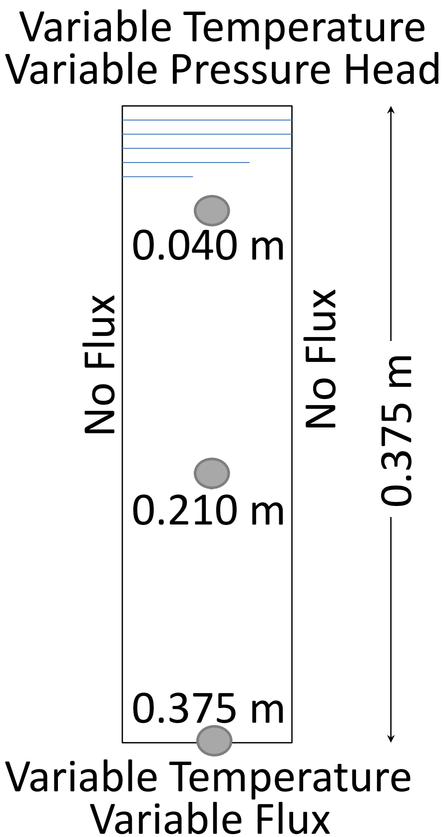

Fig. 4. Hydrus 1-D numerical model domain and prescribed boundary conditions.

HESSD
9, 4305–4332, 2012

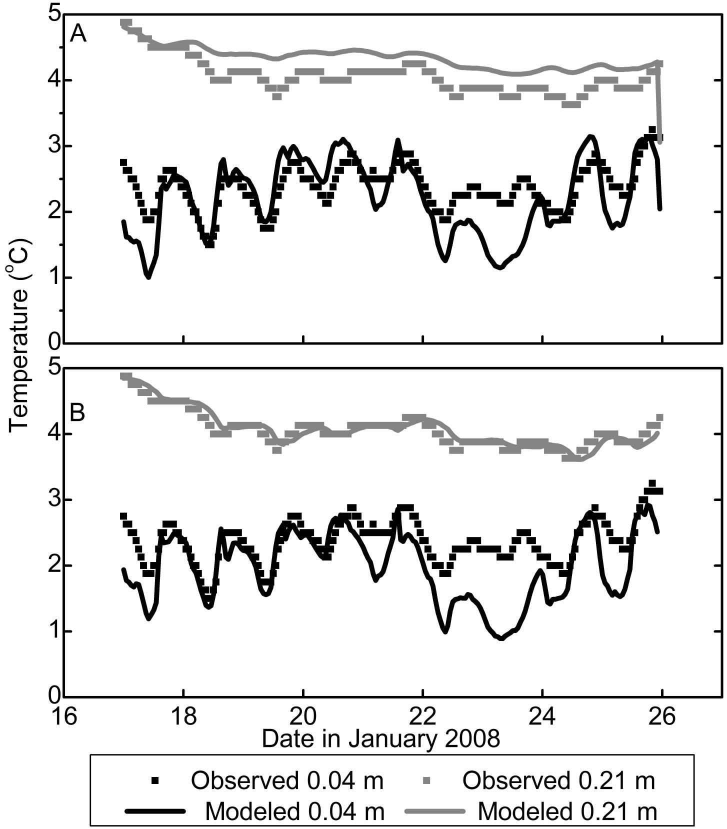

Fig. 5. Hydrus model results using **(A)** a constant flux through the model, and **(B)** a time-variable flux fit to both the 0.04 m and 0.21 m data at each one-hour timestep for the 9-day period.

HESSD

9, 4305–4332, 2012

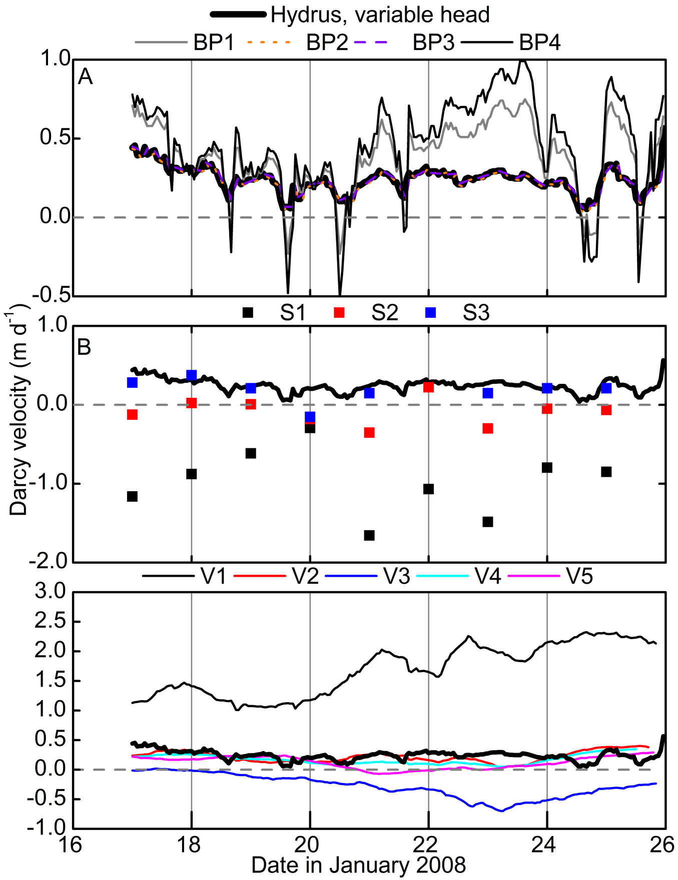

Fig. 6. **(A)** Hourly Hydrus and BP flux estimates, **(B)** daily HK flux estimates, and **(C)** hourly HK flux estimates using VFLUX. Hydrus results are plotted on **(B)** and **(C)** for comparison. The dashed gray line indicates no flux; positive flux indicates upward water movement whereas negative flux is downward water movement.

HESSD
9, 4305–4332, 2012

Estimation of upward flux through streambed sediments

M. Shanafield et al.